



Relation between regional drought and mountain dust deposition revealed by a 10-year record from an alpine critical zone



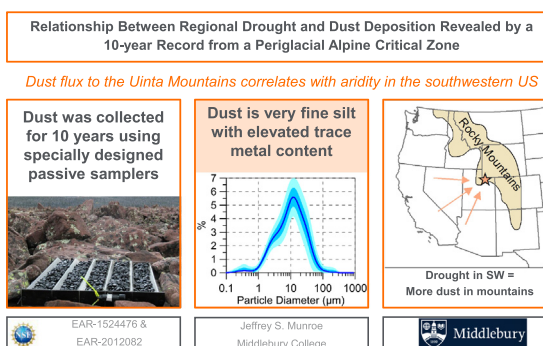
Jeffrey S. Munroe

Geology Department, Middlebury College, Middlebury, VT 05753, USA

HIGHLIGHTS

- Dust flux to the Uinta Mountains is significantly correlated with regional aridity.
- Dust is primarily very fine silt.
- Dust contains elevated abundances of trace metals.
- Average dust flux from 2011 to 21 was $3.4 \text{ g/m}^2/\text{yr}$.

GRAPHICAL ABSTRACT



ARTICLE INFO

Editor: Jianmin Chen

Keywords:

Dust
Critical zone
Drought
Uinta Mountains

ABSTRACT

Mineral dust was collected with a network of passive samplers in the Uinta Mountains (Utah, USA) over a 10-year period to evaluate the relation between regional drought and dust deposition. A total of 72 samples from eight collectors were analyzed for flux, grain size distribution, mineralogy, geochemistry, and their Sr and Nd isotopic fingerprint. The dust is primarily very fine silt, with an average median grain size of $11.6 \mu\text{m}$. The clay minerals illite and kaolinite are common in the dust, along with quartz, potassium feldspar, and plagioclase. The most abundant elements (after Si) are $\text{Al} > \text{Fe} > \text{K} > \text{Ca} > \text{Mg} > \text{Ti}$. The trace elements Cd, Sn, Sb, Zn, Cu, As, and Pb are present at abundances greatly in excess of normal levels in upper crustal rocks. Dust fluxes average $14.4 \text{ mg/m}^2/\text{day}$, generally decrease at higher elevations and toward the eastern end of the range, and are significantly higher in summer. Annual fluxes range from 1.4 to $5.8 \text{ g/m}^2/\text{yr}$ with a decadal average of $3.4 \text{ g/m}^2/\text{yr}$. Rates of dust deposition are significantly correlated with regional drought severity from the Standardized Precipitation-Evapotranspiration Index (SPEI) for the southwestern US over 2, 3, and 6-month time scales. Previous work has demonstrated a connection between drought in the southwestern US and the abundance of fine ($\text{PM}_{2.5}$) material aloft. This work is the first to use long-term monitoring of annual dust deposition to confirm that the flux of silt-sized dust to mountain ecosystems is significantly correlated with regional drought severity.

1. Introduction

The entrainment, transport, and redeposition of mineral dust are significant processes within the functioning of the Critical Zone (CZ), defined as the “dynamic interface between the solid Earth and its fluid envelopes” (National

Research Council, 2001; Shao et al., 2011). Sparsely vegetated landscapes in dryland regions are typically mantled by fine-grained mineral material in the form of loose sediment and soils (Watson, 1992). Where windspeeds and particle sizes are appropriate, mineral grains are entrained from these surfaces as suspended load and carried away (Shao, 2001; Shao and Lu, 2000). Natural and anthropogenic disturbances – including flooding, fire, agriculture, grazing, off-road vehicle travel, road construction, and extraction of fossil fuel and mineral resources – that alter the ground surface in

E-mail address: jmunroe@middlebury.edu.

these settings can greatly increase the abundance of fine-grained material available for deflation (Belnap, 1995; Neff et al., 2008; Painter et al., 2007; Wilshire, 1983). Desiccation of terminal lakes as a result of climate change and water diversions also exposes extensive areas of fine sediments to wind erosion (Borlina and Rennó, 2017; Gill, 1996; Goudie, 2018; Reheis, 1997; Wurtsbaugh et al., 2017). The result is a loss of mineral material from specific locations on the landscape.

Once aloft, dust can be transported regionally (Neff et al., 2008; Nicoll et al., 2020; Reynolds et al., 2013) and extra-regionally, i.e. beyond the immediately surrounding region (Aarons et al., 2019; Abouchami et al., 2013; Bozlaker et al., 2019; Prospero, 1999; VanCuren and Cahill, 2002). During transport, dust plays a crucial role in the formation of clouds (Froyd et al., 2022) and the generation of precipitation (Ault et al., 2011; Creamean et al., 2013; Tobo et al., 2019). In areas of focused dust entrainment, dust obscuration can influence the amount of sunlight reaching the ground surface (Kaufman et al., 2001). The capacity of dust and other aerosols to partially counteract the positive radiative forcing induced by rising atmospheric greenhouse gas concentrations makes them a critical component of Earth's radiation budget (Zhai et al., 2021).

Significant impacts to the CZ occur when dust returns to the ground, either as dry deposition or as wet deposition associated with precipitation (Bergametti and Forêt, 2014). Effects of dust deposition on soil development have long been recognized in desert (Reheis and Kihl, 1995; Yaalon and Ganor, 1973) and tropical environments (Chadwick et al., 1999; Dia et al., 2006; Dymond et al., 1974; Kurtz et al., 2001), but recent studies have illuminated the important role of dust deposition in mountain ecosystems. In particular, dust deposition alters the pH and chemistry of surface water (Brahney et al., 2013; Brahney et al., 2014; Carling et al., 2012; Psenner, 1999), contributes to soil formation (Dahms, 1993; Lawrence et al., 2011; Lawrence et al., 2013; Muhs and Benedict, 2006; Tsai et al., 2021), delivers important nutrients for plant growth and aquatic productivity (Aciego et al., 2017; Arvin et al., 2017; Ballantyne et al., 2011; Brahney et al., 2014; Lawrence et al., 2013; Scholz and Brahney, 2022), and decreases the albedo of snow, altering the timing of snowmelt (Painter et al., 2007; Painter et al., 2010; Skiles et al., 2018). Because of the significant ecosystem services provided by mountains, including fresh water and timber, wildlife habitat, and their role as recreational destinations and economic engines, impacts of dust deposition on the mountain CZ have considerable societal relevance (Egan and Price, 2017; Grêt-Regamey and Weibel, 2020; Grêt-Regamey et al., 2012).

Previous work has demonstrated a correspondence between drought and atmospheric dustiness (e.g. Hamzeh et al., 2021; Prospero and Lamb, 2003; Prospero and Nees, 1977; Zoljoodi et al., 2013), and studies in the southwestern US have documented that amounts of fine ($PM_{2.5}$) material aloft tend to be elevated under enhanced drought conditions (Achakulwisut et al., 2018; Wang et al., 2017). The number of dust deposition events at a site in southwestern Colorado was also greater during a winter with more acute drought in neighboring source regions (Painter et al., 2007). On the other hand, a connection between regional drought and annual dust flux to mountain environments has not been directly investigated, and some studies have reported the lack of a strong relation between greater amounts of particulate in the air and mountain dust deposition (Lawrence et al., 2010). As a result, not enough is known about relations between dryland climate and dust delivery to downwind mountain ecosystems.

Exacerbating this lack of knowledge is the fact that most studies of mountain dust have operated over relatively short (<2 years) times scales (e.g. Aarons et al., 2019; Heindel et al., 2020; Lawrence and Neff, 2009; Rea et al., 2020), and many relied solely on dust collected from snow (e.g. Lawrence et al., 2010; Skiles et al., 2015), limiting their implications to the winter. Continuous multi-year collections of dust have been made in other locations (e.g. Prospero, 1999), and records of past dust deposition have been developed from mountain sedimentary archives (e.g. Arcusa et al., 2020; Munroe et al., 2021a; Routson et al., 2019; Wagenbach et al., 1996). Yet long records of dust inputs to the mountain CZ have not been developed from direct systematic collections.

Here I present a decadal-scale record of dust deposition in an alpine ecosystem in the Rocky Mountains downwind of major dust emitting landscapes. Samples were subjected to a consistent series of laboratory analyses to characterize flux, mineralogy, and geochemistry. Separate summer and winter collections provide the opportunity to compare dust properties on seasonal timescales. Dust flux and properties were then compared with the Standardized Precipitation-Evapotranspiration Index (SPEI) for the southwestern US. The overall hypothesis tested is that dust flux to the mountain CZ, and properties of that dust, are regulated by aridity in the southwestern US.

2. Study design

Fieldwork for this project was conducted in the Uinta Mountains (hereafter, the "Uintas"), a Laramide-age uplift of Precambrian siliciclastic rocks in northeastern Utah, USA (Fig. 1A). The highest elevations of the Uintas were above the limit of alpine glaciers during the Pleistocene (Munroe and Laabs, 2009). As a result, extensive areas of this environment feature gently sloping landscapes mantled by alpine tundra (Munroe, 2006) that have been evolving under periglacial conditions for timescales of 10^6 years or longer (Munroe et al., 2021b). Soils of this upland have been strongly influenced by dust deposition, which has created a cap of loess and contributed to the overall soil mineralogy (Bockheim and Koerner, 1997; Bockheim et al., 2000; Munroe, 2007; Munroe et al., 2015; Munroe et al., 2020; Munroe et al., 2021b). The role of these dust-influenced soils in controlling water chemistry in the Uintas has been documented by recent studies (Checketts et al., 2020; Hale et al., 2022).

Purpose-built passive samplers were used to investigate the properties of modern dust accumulating in the Uintas (Munroe, 2014; Munroe et al., 2015; Munroe et al., 2019). The collectors are based on the marble dust trap typically used in dryland research (e.g. Reheis and Kihl, 1995; Wesley and Hicks, 2000; Sow et al., 2006), modified for use in this higher precipitation environment. Collectors are a clear polycarbonate tray measuring 56×56 cm by 7.5 cm deep (Fig. 1B) that is divided into 5 "V-shaped" troughs, each of which is filled with ~ 400 , 1.75-cm diameter glass beads (~ 7 kg per collector). The beads form a rough surface that traps dust from the air, protects previously deposited dust from the wind, and reduces the possibility of dust splashing out during precipitation events. The troughs inevitably collect water as well as dust, but the black beads heat in the sun to evaporate water between precipitation events. If the troughs completely fill, a row of small (3 mm) holes allows water to trickle out. Dust trapped by the beads settles to the base of each trough where it remains as water evaporates. Technical build sheets detailing the dimensions, materials, and part numbers for the collectors are presented in the Supplemental Materials.

The first four collectors (DUST-1 through DUST-4) were deployed in June of 2011, and four more (DUST-5 through DUST-8) were added in the fall of 2015 (field photographs of each are provided in the Supplemental Materials). All were positioned above treeline at elevations greater than ~ 3400 m asl (Fig. 1A, Supplemental Table 1). As required by the US Forest Service in exchange for permission to conduct this study, the collectors were deployed on the ground surface. Dust is rinsed from a collector with distilled water, typically in early summer (a "winter" sample, \sim October through June) and in fall (a "summer" sample, \sim June through October). By compositing multiple dust delivery events, this strategy provides a perspective midway between event-scale sampling, such as dust on snow layers (e.g. Lawrence et al., 2010; Skiles et al., 2018) and plume tracking with remote sensing (Hahnenberger and Nicoll, 2014), and the long-term averaging provided by soil (Lawrence et al., 2011) and lake sediment (Arcusa et al., 2020; Munroe et al., 2021a; Neff et al., 2008) studies.

A total of 13 field visits were made to the Uintas in order to remove dust from the collectors. The original four collectors were deployed in the summer of 2011, and visited again in September 2011, July 2012, June 2013, July 2014, July 2015, October 2015, and July 2016. Three of these four were visited again October 2016 (DUST-4 was inaccessible due to snow), and the second set of four collectors was deployed. Return visits were

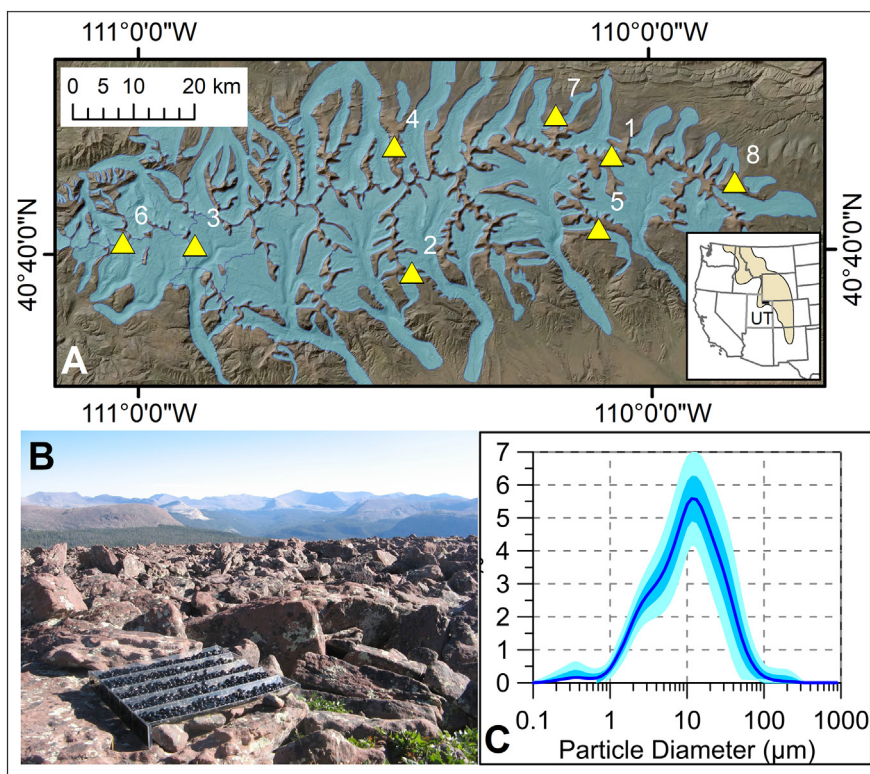


Fig. 1. (A) Locations of the 8 passive dust collectors (yellow triangles) in the Uinta Mountains. Blue polygons represent the extent of glacier ice at the Last Glacial Maximum (Munroe and Laabs, 2009). Inset shows the location of the Uinta Mountains (box) in the state of Utah (UT) in the western United States. (B) Representative photograph of a passive dust collector (DUST-2). (C) Average grain size distribution (dark blue) of Uinta dust samples ($n = 72$) collected between 2011 and 2021. Shades of blue represent 1- σ and 2- σ ranges.

then made in June 2017, September 2019, September 2020, June 2021, and October 2021. Visits that were spaced \sim one year apart yielded an annual sample. The summer and fall visits in 2011, 2012, 2015, 2016, and 2021 collected dust from specific seasons. The long interval from 2017 to 2019 merged three summers and two winters. It was not always possible to visit each collector during each trip; in some years, late-lying snow, fires, road closures, and other challenges precluded access to specific sites. DUST-1 and DUST-3 were visited the most, at 13 times each (Supplemental Table 1). DUST-7, which was destroyed by the wind and later replaced in the same location, was visited the fewest number of times (5). The overall dataset consists of 72 samples from 13 different collections, each involving from 2 to 8 collectors (Supplemental Table 1).

3. Analytical methods

At Middlebury College, dust was concentrated by centrifugation, treated with 35 % H_2O_2 (\sim 5–10 days) to remove organic matter, and sieved to $63 \mu\text{m}$ to remove sand-sized particles assumed to be locally sourced. The grain size distribution of these samples was then analyzed with laser scattering in a Horiba LA950-v2. This instrument has an effective range from 10 nm to 3 mm, and a refractive index of 1.54 with an imaginary component of 0.1i was used in the calculating the grain size distribution on a volume basis. Massing of the samples after oven drying at 60°C permitted calculation of dust flux in $\text{mg}/\text{m}^2/\text{day}$.

The mineralogy of the samples was analyzed on a Bruker D8 Advance Model X-Ray Diffractometer (XRD). The instrument was operated at 40 kV and 40 mA with a solid-state detector, theta-theta goniometer, and $\text{CuK}\alpha$ radiation. Samples were scanned as oriented powders from 2 to $40^\circ 2\theta$. Mineral spectra peaks were identified by visual comparison with standard reference patterns.

The abundances of various major and trace elements in the dust samples were determined by Inductively Coupled Plasma Mass Spectrometry (ICP-

MS) at Middlebury College and different external laboratories over the ten-year period. Appropriate reference materials and internal standards were incorporated in all analytical runs to permit inter-comparison. In compiling the dataset discussed in this paper, only elements quantified in $>85\%$ of the dust samples were considered. The resulting dataset includes 44 elements quantified for 70 separate samples. Principle component analysis was conducted for the major elements using a varimax rotation to aid interpretation of the geochemical dataset.

Dust samples were analyzed for Sr and Nd isotopes in the Department of Geosciences at the University of Wisconsin-Madison. A detailed methodology for these analyses was presented in prior work (Munroe et al., 2019). Briefly, samples were dissolved in concentrated HF and HNO_3 , followed by HCL. Cation exchange columns were used to isolate Sr and rare earth elements. Strontium was analyzed by Thermal Ionization Mass Spectrometry (TIMS) with exponential normalization to an $^{86}\text{Sr}/^{88}\text{Sr} = 0.1194$, and Nd was analyzed by multi-collector ICP-MS with exponential normalization to a constant $^{146}\text{Nd}/^{144}\text{Nd}$ of 0.7219. Following convention, Nd isotope compositions are presented as $\epsilon_{\text{Nd}} = \left(\frac{(^{143}\text{Nd}/^{144}\text{Nd})_{\text{sample}}}{(^{143}\text{Nd}/^{144}\text{Nd})_{\text{CHUR}}} - 1 \right) \times 10^4$, where CHUR is the chondritic uniform reservoir value of 0.512638 ± 0.000005 (Bouvier et al., 2008).

Drought conditions for the past ten years were constrained by the Standardized Precipitation-Evapotranspiration Index (SPEI) for a region stretching from the northwest corner of Nevada (42.25°N , 120.25°W), southeastward to the midpoint of the Arizona/New Mexico border (34.25°N , 109.25°W). Monthly average values of the SPEI for this region spanning 1, 2, 3, 6, 12, and 24 months were processed from data obtained from <https://spei.csic.es/>. Mean values for these intervals were determined for the duration of each dust collection to constrain hydroclimate conditions in regional dust source areas. The correlation between SPEI metrics and dust flux was evaluated with a non-parametric Spearman rank correlation test, given the skewed nature of the flux data and the size of the overall dataset.

4. Results

4.1. Dust properties

Dust in the Uintas has a consistent grain size distribution from site to site, and from year to year (Fig. 1C, Supplemental Table 2), with an overall median of 11.6 μm ($\sim 6.5\phi$). Very fine silt (7.8–15.6 μm) is the most abundant size class (27 %, by volume). Mineralogically, the dust consists of quartz, plagioclase, K-feldspar, and illite with trace amounts of kaolinite, chlorite, and amphibole. The most abundant rock-forming elements (after Si) are Al (7.0 %), Fe (3.1 %), K (2.5 %), Ca (1.1 %), Mg (1.1 %), and Ti (0.4 %) (Supplemental Table 3). Trace elements present at >100 ppm include Ba, Mn, Zn, Zr, Sr, Cu, and Rb (Supplemental Table 3). Principle component analysis of the major elements loads Mg, Al, and Fe on PC-1; Mn, Ca, and K on PC-2; and Ti on PC-3, with a complicated pattern of variability between sites and seasons (Supplemental Fig. 2). When normalized to Al, and compared to normal crustal abundances (Wedepohl, 1995), the elements Cd, Sn, Sb, Zn, Cu, As, and Pb have average enrichments $>5\times$ (Fig. 2). The ratio $^{87}\text{Sr}/^{86}\text{Sr}$ in most Uinta dust samples clusters tightly between 0.711 and 0.718; values of ϵ_{Nd} are similarly grouped between -9 and -11.5 (Fig. 3, Supplemental Table 4).

4.2. Dust fluxes

For the period of record, dust fluxes average 14.4 $\text{mg}/\text{m}^2/\text{day}$, excluding a single sample (DUST-8, summer 2021) with an exceedingly high value attributed to local surface disturbance (Fig. 4). Fluxes generally decrease at higher elevations and are greater at the western end of the range. Daily fluxes vary from year to year, but generally exhibit a similar pattern within each collection (Fig. 5). Annual fluxes range from 1.4 to 5.8 $\text{g}/\text{m}^2/\text{yr}$ with an overall average for the decade of 3.4 $\text{g}/\text{m}^2/\text{yr}$.

4.3. Temporal and spatial contrasts

The pairs of winter/summer samples support consideration of dust properties on seasonal timescales. Summer dust is significantly finer than winter dust (median of 8.3 vs. 10.1 μm , $P < 0.001$), driven by a reduced component of medium silt (Supplemental Table 5). Daily dust fluxes are significantly ($P < 0.001$) higher in summer (27 vs. 9 $\text{mg}/\text{m}^2/\text{day}$) (Fig. 5 inset, Supplemental Table 5). Abundances of Ba, Ca, Cd, Fe, Mn, Ni, Pb, Sn, and Tb are significantly greater ($P < 0.05$) in summer dust (Supplemental Table 6), whereas K is significantly more abundant in the winter (Fig. 6). There is no difference between PC-1 in summer vs. winter, but PC-2 is significantly greater in summer dust, likely due to Ca within plagioclase feldspar. In three of the four years, $\sim 40\%$ of the dust by mass accumulated during the summer months, and 60 % in winter, but in 2016–17 the proportion was closer to 50:50.

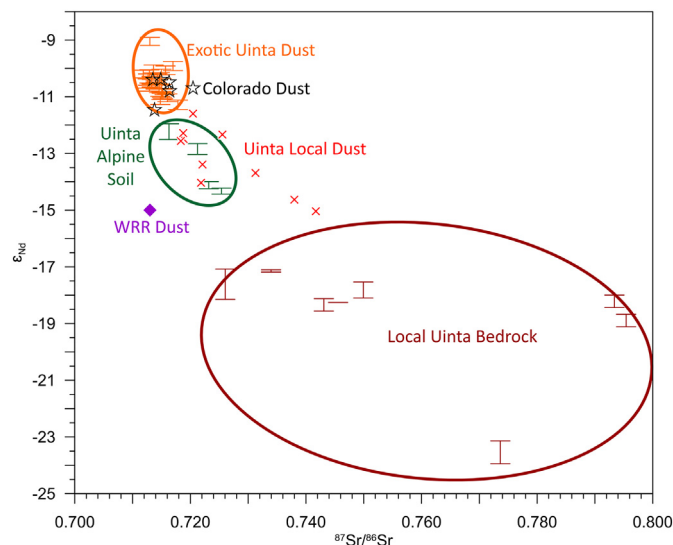


Fig. 3. Biplot of $^{87}\text{Sr}/^{86}\text{Sr}$ and ϵ_{Nd} in Uinta dust, alpine soil, and rock samples. Samples of exotic Uinta dust cluster tightly with $^{87}\text{Sr}/^{86}\text{Sr}$ between 0.711 and 0.718 and ϵ_{Nd} between -9 and -11.5 (orange ellipse). Uinta bedrock samples (dark red) exhibit considerably more radiogenic $^{87}\text{Sr}/^{86}\text{Sr}$ and more negative ϵ_{Nd} , whereas alpine soil samples (green) are a mixture of the two end members (Munroe et al., 2020). Exotic Uinta dust samples have a similar isotopic fingerprint to dust (black stars) reported from southwestern Colorado (Ballantyne et al., 2011; Lawrence et al., 2011; Neff et al., 2008; Painter et al., 2007), but have higher ϵ_{Nd} values than a dust sample (purple diamond) reported from the Wind River Range of (WWR) Wyoming (Brahney et al., 2014). Some Uinta dust samples (red crosses) apparently contain local material that has influenced their isotope fingerprint.

The composition of Uinta dust is generally similar from site to site and year to year, with some notable exceptions. Spatially, values of PC-1 (Al, Fe, Mg) are lower in the two collectors at eastern end of the range (DUST-7 and DUST-8). PC-3 (Ti) is highest in the westernmost collector (DUST-6) but fairly consistent elsewhere. In terms of trace elements, Sn and W are more common at the west end, and Pb at the east end. Some of the elements significantly more abundant in summer dust, for instance Ba and Ca, are deposited in greater amounts across the south side of the range. In contrast, K, which is more abundant in winter dust, tends to be more common in dust deposited on the north side.

Year to year variability is noted in some elemental ratios; for instance Ti/Zr had elevated values in the collections between 2011 and 2013 (reaching peak values in the 2012–13 annual sample), and lower and relatively constant values from 2015 to the end of the record. Values of Rb/Sr and Th/U were also highest in the first few years of the dataset. In contrast, La/Th was highest in the summer of 2015 and lowest in the final year.

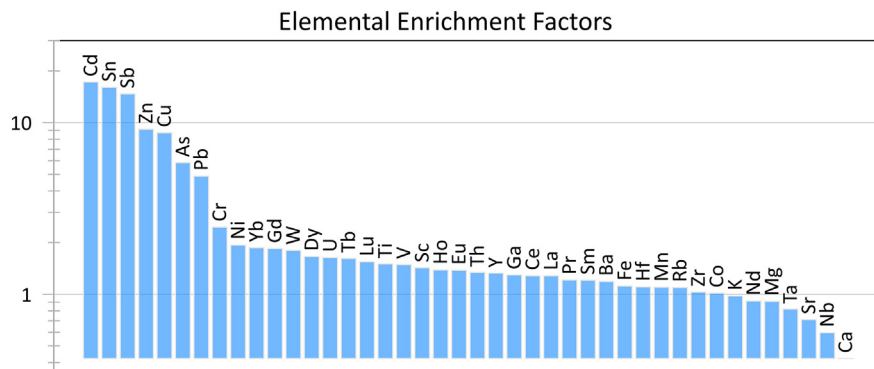


Fig. 2. Average enrichment factors of major and trace elements measured in Uinta dust samples. Values were computed as (Element/Al) relative to (Element/Al) in average upper continental crust (Wedepohl, 1995). Note the logarithmic scale on the Y-axis.

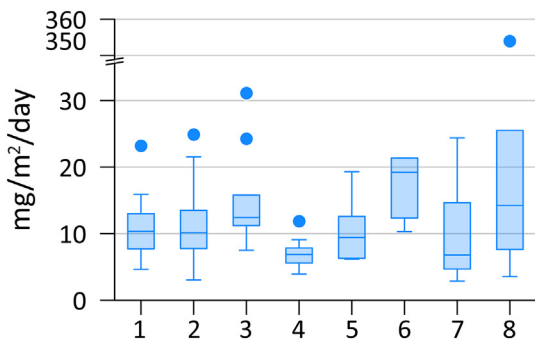


Fig. 4. Box and whisker plot displaying the range of dust fluxes (in $\text{mg}/\text{m}^2/\text{day}$) at the 8 Uinta dust collectors. Collectors 1–4 were deployed in 2011; collectors 5–8 were added in 2015. Horizontal lines represent median values, box represents interquartile range, whiskers represent interquartile range $\times 1.5$, and dots represent outliers. Note the Y-axis is broken to permit plotting of the outlier for the summer of 2021 at DUST-8, a sample likely influenced by local disturbance.

5. Discussion

5.1. Uniqueness of the record

The duration of the Uinta dust record greatly exceeds any previously published dust collection effort in a mountain setting. Early work in the Wind River Mountains of Wyoming, for example, collected dust over a two year period (Dahms and Rawlins, 1996). Extensive work on dust deposition in the San Juan Mountains of Colorado involved collection over five years, but focused only on dust deposited during the winter (Lawrence et al., 2010). More recent studies presented a one-year record of dust deposition along an elevation gradient on the east side of the Colorado Rockies (Heindel et al., 2020), a one-year record from the Sacramento Mountains of New Mexico (Rea et al., 2020), and three-month collections of dust on the western side of the Sierra Nevada in California (Aarons et al., 2019). In this context, the 10-year record from the alpine zone of the Uintas is singular.

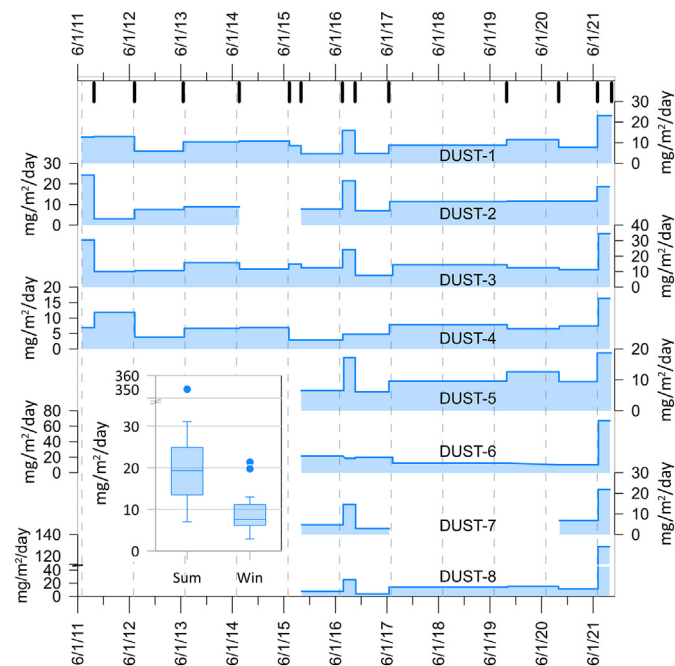


Fig. 5. Timelines of dust flux at the Uinta collectors in $\text{mg}/\text{m}^2/\text{day}$ through the entire period of record. Thick black lines at the top denote collections, whereas vertical dashed lines mark July 1 each year to highlight the start of summer. Inset shows dust flux by season, highlighting the significantly greater flux in summer vs. winter.

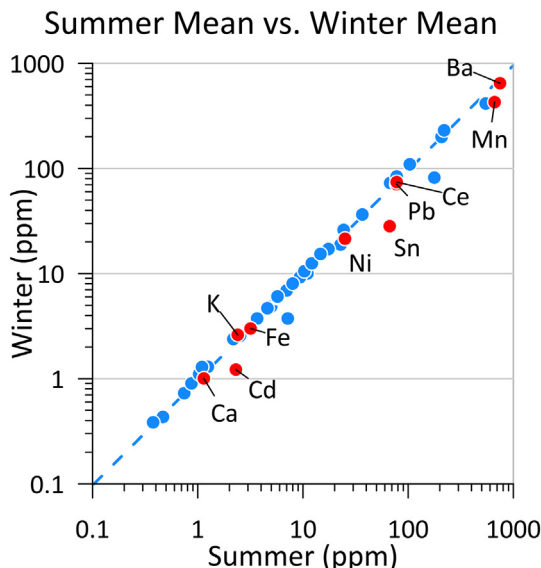


Fig. 6. Average values of major and trace elements in seasonal (winter/summer) pairs of Uinta dust samples. Elements plotted in red are significantly more abundant in summer (Ca, Cd, Fe Ni, Sn, Pb, Ce, Mn, Ba) or winter (only K).

Furthermore, most previous studies deployed collectors at a relatively small number of sites; such as two in the Sacramento Mountains (Hale et al., 2022), and four in the Sierra Nevada (Aarons et al., 2019), in contrast to the eight locations in the Uintas. Some studies have utilized larger numbers of samplers, for example nine in the Colorado Rockies, but intentionally spread them out over a large elevation range (Heindel et al., 2020). Other projects involved numerous collectors, for instance 15 sites in western Utah (Goodman et al., 2019) or 55 sites in southern Nevada and California (Reheis and Kihl, 1995), but focused on relatively low elevations. The Uinta collector network, therefore, is unique in that it was intentionally designed to provide a large amount of information specifically about modern dust deposition in a high mountain setting during both summer and winter seasons. This distinction supports use of the Uinta dataset in evaluating connections between dust properties and regional climate.

5.2. Dust properties

The average median grain size ($11.6 \mu\text{m}$) of Uinta dust (Fig. 1C, Supplemental Table 2) suggests that this material is intermediate between regional (typically $>10 \mu\text{m}$) and far-traveled dust (typically $<10 \mu\text{m}$), or is a mixture of the two (Aarons et al., 2016; Mahowald et al., 2005; Neff et al., 2008). This dust, therefore, straddles the “large” (i.e. local) and “small” (i.e. far-traveled) dust categories presented by previous work (Stuut et al., 2009) and resembles an identified end member in studies of Chinese loess records (Vandenberghe, 2013). Notably, Uinta dust has a finer modal size ($11 \text{ vs. } \sim 50 \mu\text{m}$) than material described from the San Juan Mountains of Colorado, immediately downwind of the Colorado Plateau (Lawrence et al., 2010; Neff et al., 2008). On the other hand, the Uinta dust is somewhat coarser than samples of dust deposited in the past two centuries that were analyzed from a high-elevation ice core in the Wind River Mountains (Aarons et al., 2016). The general consistency of the grain size distribution from site to site illustrates the well-mixed nature of this eolian sediment.

Mineralogically, the variety of phases present in Uinta dust is similar to other reports from the region, with abundant quartz, potassium and plagioclase feldspar, and the clay minerals kaolinite and illite (Lawrence et al., 2010). Significantly, this composition greatly exceeds the mineralogical simplicity of the Uinta bedrock, which is dominated by quartz with minor amounts of K-feldspar (Munroe, 2014). This contrast underscores the importance of dust deposition as a contribution to soil development in these mountains (Bockheim and Koerner, 1997; Bockheim et al., 2000; Munroe et al., 2020; Munroe et al., 2021b), as has been reported for other mountain

settings in the American West (Birkeland et al., 1987; Dahms, 1993; Litaor, 1987; Muhs and Benedict, 2006; Thorn and Darmody, 1980).

The geochemistry of Uinta dust generally resembles other analyses of mountain dust reported from the region (Supplemental Table 3). In terms of major elements, Al, Fe, K, and Mg are abundant in Uinta dust at concentrations similar to values reported for the San Juan Mountains and the Front Range in Colorado (Heindel et al., 2020; Lawrence et al., 2010). On the other hand, the abundance of Ca is similar between the Uintas and the Colorado Front Range, but is much higher in the San Juan Mountains (Supplemental Table 3), likely due to proximity to carbonate rocks on the Colorado Plateau. For trace elements, Pb is notably more abundant in Uinta dust compared to sites in Colorado, perhaps reflecting emissions from urban areas in northern Utah. Cu and Co are considerably more abundant in Uinta dust compared with the Colorado Front Range, but are present at concentrations similar to the San Juan Mountains. This pattern may reflect fugitive dust from hard-rock mining operations (Reynolds et al., 2010).

It is also notable that abundances of many heavy metals are highly elevated in Uinta dust (Fig. 2), a pattern that has been reported by previous work and interpreted as evidence that anthropogenic activities have altered the composition of eolian dust in this region (Carling et al., 2012; Heindel et al., 2020; Lawrence and Neff, 2009; Munroe, 2014; Munroe et al., 2015). All of the elements in Uinta dust with abundances $>5\times$ average crustal levels (Cd, Sn, Sb, Zn, Cu, As, and Pb) were shown in lake sediment records from the Uintas to have increased in the middle to late 1800s, a rise attributed to mining and smelting in the Wasatch Range immediately to the west (Reynolds et al., 2010).

Because of their constancy in the face of chemical weathering, the ratio $^{87}\text{Sr}/^{86}\text{Sr}$ and the value ϵ_{Nd} are typically used as fingerprints for identifying dust source regions (e.g. (Pourmand et al., 2014; Zhao et al., 2018)). The generally consistent range of $^{87}\text{Sr}/^{86}\text{Sr}$ and ϵ_{Nd} determined for Uinta dust (Fig. 3, Supplemental Table 4), therefore, indicates that the same source areas contribute year after year, with variability reflecting changes in the relative abundance of different source areas. The few samples that fall outside the tightly clustered range (Fig. 3) likely contain material derived from the area immediately surrounding the samplers (Munroe et al., 2019). Nonetheless, average values of $^{87}\text{Sr}/^{86}\text{Sr}$ and ϵ_{Nd} are similar to those reported from Colorado (Ballantyne et al., 2011; Lawrence et al., 2011; Neff et al., 2008) and Wyoming (Aarons et al., 2016). Ratios of $^{87}\text{Sr}/^{86}\text{Sr}$ in Uinta dust also overlap with those measured for playa sediments in western Utah and dust in the Wasatch Mountains (Carling et al., 2020; Miller et al., 2014; Munroe et al., 2019). On the other hand, ratios of $^{87}\text{Sr}/^{86}\text{Sr}$ in Uinta samples are more radiogenic than dust reported from California (Aarons et al., 2019) or the gypsum-bearing dust reported from New Mexico (Rea et al., 2020), both of which have ratios 0.708 to 0.710. Uinta dust samples also have higher values of ϵ_{Nd} than a dust sample (Fig. 3) reported from the Wind River Range (Brahney et al., 2014). These differences indicate that at least some of the dust arriving in the Uintas is coming from different sources than the dust analyzed in these other studies.

5.3. Dust fluxes

The dust fluxes measured for the Uintas are similar to the range of 0.1 to 11.3 g/m²/yr reported for the Wind River Range in Wyoming (Dahms and Rawlins, 1996), and 5.9 to 18.9 g/m²/yr on the eastern slope of the Colorado Rockies (Heindel et al., 2020). Higher fluxes have been reported for sites farther to the southeast in Colorado (Lawrence et al., 2010) and New Mexico (Rea et al., 2020). Previous work has demonstrated that dust fluxes are generally lower at higher elevations (Heindel et al., 2020), thus the lower values in the Uintas may reflect a combination of greater distance from prominent dust source regions and the position of the Uinta collectors at elevations higher than in previous studies. Furthermore, values for the Uintas are likely underestimates given the imperfect efficiencies of marble collectors (Sow et al., 2006). Nonetheless, at the average flux of 3.4 g/m²/yr, ~1500 metric tons (1.53×10^9 g) of dust accumulates annually across the ~450 km² of alpine terrain in the Uintas (Munroe, 2006).

5.4. Drivers of seasonal contrasts

Differences between winter and summer dust are attributed to climatic contrasts between these seasons. Data from the Chepeta remote automated weather station (RAWS) on the crest of the Uintas (3694 m) reveal that average wind speeds at high elevations in the Uintas are higher during winter months (Munroe et al., 2019), which is consistent with the coarser mean grain size of winter dust. NW winds are also dominant in during the time when the winter samples accumulate, with southerly winds in summer (Munroe et al., 2019). The greater abundances of several elements in the summer dust (Fig. 6, Supplemental Table 6), therefore, suggest that their major sources are located to the south of the Uintas. The variation noted in the elemental ratios Ti/Zr, Th/U, Rb/Sr, and La/U, is a further demonstration that different dust source regions are dominant in contributing dust to the Uintas in different seasons, and sometimes between different years.

5.5. Dust flux relation to drought severity

The decade in which the dust collectors were deployed featured wide ranges in hydroclimate superimposed on an overall persistent drought regime (Williams et al., 2022). The overall average SPEI, for 1 to 24-month intervals, was negative for the decade (Supplemental Fig. 2). Maximum SPEI values for shorter time intervals (≤ 3 months) reach ~1.5, yet they decrease for longer intervals, and for at the 24-month interval, the maximum is ~0 (Supplemental Fig. 2). Minimum values reach -2 or lower, classified as “extremely dry” (Dikshit et al., 2021). At the scale of individual collections, SPEI values were nearly always negative, reaching particularly low values for the annual 2012–13 sample, the winter 2020–21, and the summer 2021 (Supplemental Table 7).

It is logical that dust flux in the Uintas would correspond with the intensity of drought experienced by the southwestern US as a whole, a region of expansive arid landscapes that hosts numerous known dust sources (Hahnenberger and Nicoll, 2014; Hahnenberger and Perry, 2015; Miller et al., 2012; Neff et al., 2008; Painter et al., 2007). Indeed, the highest values of dust flux for the entire record were attained in the summer of 2021 when soil moisture in the southwest was exceptionally low (Williams et al., 2022) and SPEI values for the region considered in this study were low immediately following a dry winter (SPEI-6 values < -1.00).

Although there is scatter in the data, reflecting the variable number of samplers emptied with each collection, overall ranked dust flux exhibits a significant negative correlation (Fig. 7) with ranked SPEI-2 (-0.244 , $P = 0.039$), SPEI-3 (-0.253 , $P = 0.032$), and SPEI-6 (-0.252 , 0.033). Relationships with longer (SPEI-12 and SPEI-24) values also exhibit negative correlations, but these are not significant. Values of SPEI are closely connected with soil moisture (Afshar et al., 2022), with more negative values reflecting a reduced moisture level. The significant negative correlation between seasonal (2, 3, and 6 month) SPEI and dust flux (Fig. 7), therefore, confirms the hypothesis of this study that increasing drought conditions in the southwestern US (more negative SPEI values) correspond to greater deposition of mineral dust to the CZ in the Uinta Mountains.

Numerous studies have concluded that arid landscapes like the southwestern US will become drier in the future (Cayan et al., 2010; Cook et al., 2015; Seager et al., 2007; Seager et al., 2013), and the evolving megadrought in this region reinforces the current trend toward drier conditions (Williams et al., 2022). Results from this decade of dust collection in the Uintas suggest that future increases in drought severity or extent in the southwestern US will translate into higher rates of dust deposition in downwind mountains. Given the significance of dust deposition to the mountain CZ, this connection needs to be incorporated into models attempting to predict future dust in the southwestern US in general (Brey et al., 2020), and fluxes to mountain ecosystems specifically.

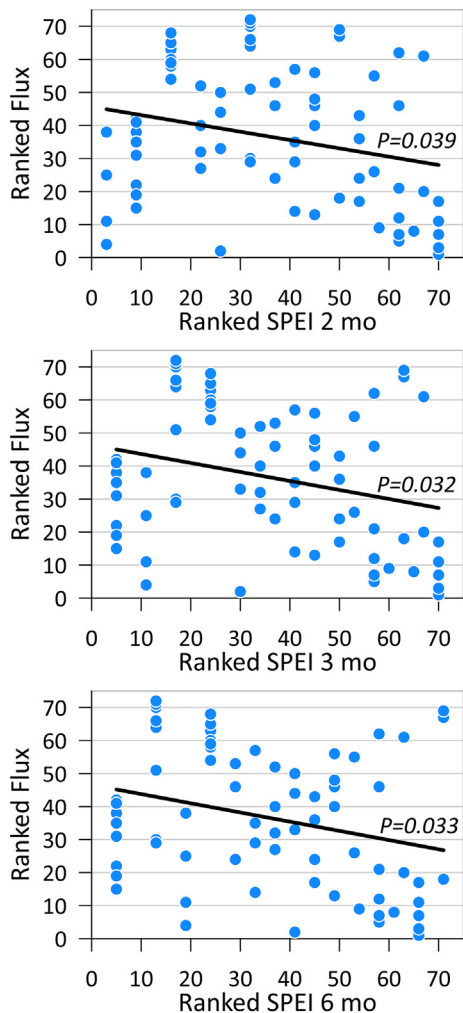


Fig. 7. Significant linear regressions between ranked SPEI metrics (2, 3, and 6 months) and ranked dust flux. *P* values from a Spearman's rank correlation are provided alongside the linear fit to the data.

5.6. The role of snow cover

Understanding the controls on dust flux to the Uintas also requires consideration of the role of winter snow cover. The Uintas are a snow-dominated system, with accumulation typically beginning in October each year, and snow cover persisting at least locally well into the following summer. Snow cover at each collector was tracked with temperature dataloggers during the winters of 2016–17 and 2020–21 revealing durations from 0 to 235 days. It is important to note that this approach provides information solely about the presence/absence of snow above the collector, not the depth or other properties of that snow. Nonetheless, in both winters the relation between snow cover duration and dust flux was positive and significant (Fig. 8). A positive correlation was also noted between dust flux and snow cover duration during the 12-month interval between fall of 2019 and fall of 2020, as well as in a multi-year collection spanning summer 2017 to fall of 2019. Multiple linear regression reveals that overall dust flux can be well predicted by a combination of snow cover duration ($P = 0.005$) and SPEI-2 ($P = 0.043$). If the duration of snow cover corresponds to snow depth, then this relation suggests that deeper snow contains more dust leading to greater dust accumulation in the collector upon meltout. Alternatively, it may be that the snow surface itself is an effective trap for dust, with longer duration of snow cover leading to greater dust capture. Either way, it is notable that duration of snow cover at a given collector in the alpine zone does not correlate in a consistent manner with snow cover

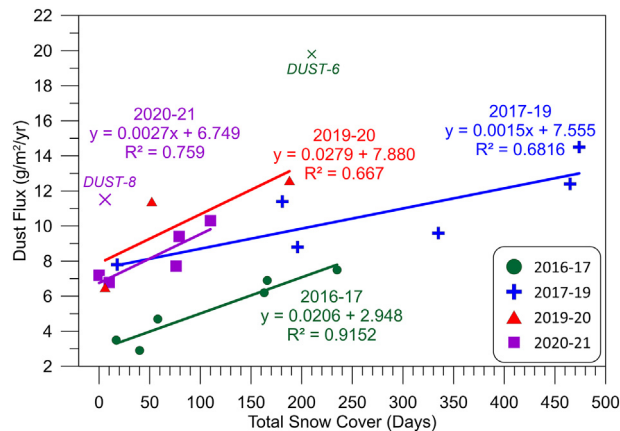


Fig. 8. Relation between duration of snow cover above a dust collector and dust flux during the winter seasons of 2016–17 and 2020–21, the 12-month interval from fall 2019 to fall 2020, and a long-duration collection spanning 2017–19. “DUST-6” and “DUST-8” mark individual samples excluded from the regressions because of local disturbance. In all cases a longer duration of snow cover corresponds to greater dust accumulation.

(depth or duration) at lower elevation SNOTEL sites. The snow cover in question, therefore, appears to be local drifting controlled by prevailing winds during specific storm events. Nonetheless, at least for the winter season, it appears that the duration of snow cover over a collector exerts an additional control on dust accumulation.

5.7. Further considerations

This work has demonstrated that dust flux to the Uinta Mountains is strongly correlated with drought conditions in the southwestern US; nonetheless, several considerations must be taken into account when interpreting this result. For instance, it is likely that at least some of the dust arriving in the Uintas is coming from beyond the southwestern US. Asian dust, for example, has been geochemically identified in dust arriving on the western slope of the Sierra Nevada in California, ~800 km to the west of the Uintas (Aarons et al., 2019; Ault et al., 2011; Creamean et al., 2013; Creamean et al., 2014) and Saharan dust has been tracked into the south-central USA (Bozlaker et al., 2019). Studies combining modeling and monitoring of airborne PM_{2.5} have also concluded that Asian dust is dominant in western North America during the spring season in areas remote from local deserts (Kim et al., 2021). If appreciable dust is reaching the Uintas from beyond the southwestern US, then knowledge of drought conditions there would fail to capture the situation in all of the relevant source areas. This possibility is difficult to evaluate definitively; however, given that the grain size distribution of Uinta dust is consistent with a regional origin (Neff et al., 2008), that isotopic fingerprints of Uinta dust have been shown to match possible source regions in the southwestern US (Munroe et al., 2019), and that remote sensing studies and back-trajectory analyses have tracked dust from the southwestern US into the Colorado Rocky Mountains (e.g. Neff et al., 2013; Painter et al., 2007; Skiles et al., 2015)), it seems unlikely that a large proportion of the silt-sized Uinta dust is derived from beyond North America.

It is also plausible that the emission of dust from a landscape is a stochastic phenomenon controlled by local factors that might not always be captured by a regional perspective like the SPEI metric. Local surface disturbance (Belnap and Gillette, 1998), interactions between frontal system passage and topography (Hahnenberger and Nicoll, 2012; Nicoll et al., 2020; Steenburgh et al., 2012), or landscape recovery after fire (Miller et al., 2012), could all drive the emission and transport of dust from a specific location. Because the Uinta collectors inevitably merge an unknown number of dust delivery events into each composite sample, it is possible that just a few events delivering dust from locations with transient yet

ideal conditions could be responsible for the majority of a sample, muting any connection between overall drought and dust flux.

It is also known that different landscapes react to drought in divergent ways that influence their role as dust sources. For instance, alluvial fans tend to emit more dust under wetter conditions, because water is required to transport fine sediment onto the fan surface. In contrast, playas tend to release more dust in dry years, unless a mineral crust forms and renders the surface resistant to wind erosion (Reheis and Kihl, 1995; Reynolds et al., 2007). This trade-off has been employed to explain the counterintuitive reduction of dust emission from the Mojave Desert during a dry interval in the middle Holocene (Tau et al., 2021). As a result, a complicated patchwork of possible dust sources across the landscape might be activated or suppressed in response to changing drought severity, obfuscating any simple or direct linkage with integrated downwind dust flux.

Despite these considerations, the conclusion that dust deposition in the Uintas is correlated with drought severity in the southwestern US extends previous work linking drought with air quality and concentrations of fine material aloft. From this ten-year record it is probable that, if regionally averaged drought conditions become more severe in the future, the flux of silt-sized material reaching the Critical Zone in downwind mountain ecosystems will increase.

6. Conclusion

On the basis of continuous collection spanning the decade 2011–2021, silt-dominated dust is accumulating in the alpine zone of the Uinta Mountains (Utah) at an average rate of 3.4 g/m²/yr. The deposition of this material, which is mineralogically and geochemically distinct from the underlying bedrock, exerts a major influence on the development of soils and overall biogeochemical cycling in this environment. Dust flux to the Uintas is greater in the summer than in winter, and is significantly correlated with drought conditions in the southwestern US over 2 to 6-month intervals. Dust accumulation during the winter is also correlated with the duration of snow cover. This study, centered on a uniquely long and spatially focused dust collection, is the first to definitively document a relation between drought in the southwestern US and the annual flux of silt-sized dust to the Critical Zone in downwind mountains.

Author statement

The author is solely responsible for all phases of this project, from conceptualization and methodology, to funding acquisition, through investigation and analysis, to writing and visualization.

Funding

This work was supported by the US National Science Foundation [EAR-1524476 and EAR-2012082], and by Middlebury College.

Data availability

Upon publication, the 10-year dust dataset for the Uinta Mountains will be available in the EarthChem repository at doi:10.26022/IEDA/112285.

Declaration of competing interest

The authors declare that they have no known competing financial interests or personal relationships that could have appeared to influence the work reported in this paper.

Acknowledgments

Thanks to E. Attwood, C. Hale, S. Lusk, R. McElroy, D. Munroe, E. Norris, S. O'Keefe, P. Olson, A. Proctor, A. Santis, E. Soderstrom, N. Stone, and L. Wasson for their assistance in the field and laboratory.

G. Carling and P. Ryan were helpful in analyzing and interpreting the dust samples. T. Desautel and E. McMahon built the dust collectors at Middlebury College, and P. McMahon drafted the technical drawings. Two anonymous reviewers provided feedback that greatly improved the manuscript. Fieldwork for this project took place in the ancestral homelands of the Ute tribe.

Appendix A. Supplementary data

Supplementary data to this article can be found online at <https://doi.org/10.1016/j.scitotenv.2022.156999>.

References

- Aarons, S.M., Aciego, S.M., Gabrielli, P., Delmonte, B., Koornneef, J.M., Uglietti, C., Wegner, A., Blakowski, M.A., Bouman, C., 2016. Ice core record of dust sources in the western United States over the last 300 years. *Chem. Geol.* 442, 160–173.
- Aarons, S.M., Arvin, L.J., Aciego, S.M., Riebe, C.S., Johnson, K.R., Blakowski, M.A., Koornneef, J.M., Hart, S.C., Barnes, M.E., Dove, N., 2019. Competing droughts affect dust delivery to Sierra Nevada. *Aeolian Res.* 41, 100545.
- Abouchami, W., Näthe, K., Kumar, A., Galer, S.J., Jochum, K.P., Williams, E., Horbe, A.M., Rosa, J.W., Balsam, W., Adams, D., 2013. Geochemical and isotopic characterization of the Bodélé depression dust source and implications for transatlantic dust transport to the Amazon Basin. *Earth Planet. Sci. Lett.* 380, 112–123.
- Achakulwisut, P., Mickley, L.J., Anenberg, S.C., 2018. Drought-sensitivity of fine dust in the US southwest: implications for air quality and public health under future climate change. *Environ. Res. Lett.* 13, 054025.
- Aciego, S.M., Riebe, C.S., Hart, S.C., Blakowski, M.A., Carey, C.J., Aarons, S.M., Dove, N.C., Botthoff, J.K., Sims, K.W.W., Aronson, E.L., 2017. Dust outpaces bedrock in nutrient supply to montane forest ecosystems. *Nat. Commun.* 8, 14800.
- Afshar, M.H., Bulut, B., Duzenli, E., Amjad, M., Yilmaz, M.T., 2022. Global spatiotemporal consistency between meteorological and soil moisture drought indices. *Agric. For. Meteorol.* 316, 108848. <https://doi.org/10.1016/j.agrformet.2022.108848>.
- Arcusa, S.H., McKay, N.P., Routsom, C.C., Munoz, S.E., 2020. Dust-drought interactions over the last 15,000 years: a network of lake sediment records from the San Juan Mountains, Colorado. *The Holocene* 30, 559–574.
- Arvin, L.J., Riebe, C.S., Aciego, S.M., Blakowski, M.A., 2017. Global patterns of dust and bedrock nutrient supply to montane ecosystems. *Sci. Adv.* 3, eaao1588.
- Ault, A.P., Williams, C.R., White, A.B., Neiman, P.J., Creamean, J.M., Gaston, C.J., Ralph, F.M., Prather, K.A., 2011. Detection of Asian dust in California orographic precipitation. *J. Geophys. Res. Atmos.* 116.
- Ballantyne, A.P., Brahney, J., Fernandez, D., Lawrence, C.L., Saros, J., Neff, J.C., 2011. Biogeochemical response of alpine lakes to a recent increase in dust deposition in the southwestern US. *Biogeosciences* 8, 2689–2706.
- Belnap, J., 1995. Surface disturbances: their role in accelerating desertification. *Environ. Monit. Assess.* 37, 39–57. <https://doi.org/10.1007/BF00546879>.
- Belnap, J., Gillette, D.A., 1998. Vulnerability of desert biological soil crusts to wind erosion: the influences of crust development, soil texture, and disturbance. *J. Arid Environ.* 39, 133–142. <https://doi.org/10.1006/jare.1998.0388>.
- Bergametti, G., Forêt, G., 2014. Dust deposition. In: Knippertz, P., Stuut, J.-B.W. (Eds.), *Mineral Dust: A Key Player in the Earth System*. Springer Netherlands, Dordrecht, pp. 179–200. https://doi.org/10.1007/978-94-017-8978-3_8.
- Birkeland, P.W., Burke, R.M., Shroba, R.R., 1987. Holocene alpine soils in gneissic cirque deposits, Colorado front range. *U.S. Geol. Surv. Bull.* 1590 E1-E21.
- Bockheim, J., Koerner, D., 1997. Pedogenesis in alpine ecosystems of the eastern Uinta Mountains, Utah, USA. *Arct. Alp. Res.* 29, 164–172.
- Bockheim, J., Munroe, J., Douglass, D., Koerner, D., 2000. Soil development along an elevational gradient in the southeastern Uinta Mountains, Utah, USA. *Catena* 39, 169–185.
- Borlina, C.S., Rennó, N.O., 2017. The impact of a severe drought on dust lifting in California's Owens Lake area. *Sci. Rep.* 7, 1–4.
- Bouvier, A., Vervoort, J.D., Patchett, P.J., 2008. The Lu–Hf and Sm–Nd isotopic composition of CHUR: constraints from unequilibrated chondrites and implications for the bulk composition of terrestrial planets. *Earth Planet. Sci. Lett.* 273, 48–57.
- Bozlaker, A., Prospero, J.M., Price, J., Chellam, S., 2019. Identifying and quantifying the impacts of Advection North African dust on the concentration and composition of airborne fine particulate matter in Houston and Galveston, Texas. *J. Geophys. Res. Atmos.* 124, 12282–12300.
- Brahney, J., Ballantyne, A., Sievers, C., Neff, J., 2013. Increasing Ca²⁺ deposition in the western US: the role of mineral aerosols. *Aeolian Res.* 10, 77–87.
- Brahney, J., Ballantyne, A., Kocielek, P., Spaulding, S., Otu, M., Porwoll, T., Neff, J., 2014. Dust mediated transfer of phosphorus to alpine lake ecosystems of the Wind River range, Wyoming, USA. *Biogeochemistry* 1–20.
- Brey, S.J., Pierce, J.R., Barnes, E.A., Fischer, E.V., 2020. Estimating the spread in future fine dust concentrations in the Southwest United States. *J. Geophys. Res. Atmos.* 125, e2019JD031735.
- Carling, G.T., Fernandez, D.P., Johnson, W.P., 2012. Dust-mediated loading of trace and major elements to Wasatch Mountain snowpack. *Sci. Total Environ.* 432, 65–77.
- Carling, G.T., Fernandez, D.P., Rey, K.A., Hale, C.A., Goodman, M.M., Nelson, S.T., 2020. Using strontium isotopes to trace dust from a drying great salt Lake to adjacent urban areas and mountain snowpack. *Environ. Res. Lett.* 15, 114035.

- Cayan, D.R., Das, T., Pierce, D.W., Barnett, T.P., Tyree, M., Gershunov, A., 2010. Future dryness in the southwest US and the hydrology of the early 21st century drought. *Proc. Natl. Acad. Sci.* 107, 21271–21276.
- Chadwick, O.A., Derry, L.A., Vitousek, P.M., Huebert, B.J., Hedin, L.O., 1999. Changing sources of nutrients during four million years of ecosystem development. *Nature* 397, 491–497.
- Checketts, H.N., Carling, G.T., Fernandez, D.P., Nelson, S.T., Rey, K.A., Tingey, D.G., Hale, C.A., Packer, B.N., Corder, C.P., Dastrup, D.B., 2020. Trace element export from the critical zone triggered by snowmelt runoff in a Montane Watershed, Provo River, Utah, USA. *Front. Water* 51.
- Cook, B.I., Ault, T.R., Smerdon, J.E., 2015. Unprecedented 21st century drought risk in the american southwest and Central Plains. *Sci. Adv.* 1, e1400082.
- Creamean, J.M., Suski, K.J., Rosenfeld, D., Cazorla, A., DeMott, P.J., Sullivan, R.C., White, A.B., Ralph, F.M., Minnis, P., Comstock, J.M., 2013. Dust and biological aerosols from the Sahara and Asia influence precipitation in the western US. *Science* 339, 1572–1578.
- Creamean, J.M., Spackman, J.R., Davis, S.M., White, A.B., 2014. Climatology of long-range transported Asian dust along the west coast of the United States. *J. Geophys. Res. Atmos.* 119, 12–171.
- Dahms, D.E., 1993. Mineralogical evidence for eolian contribution to soils of late quaternary moraines, Wind River mountains, Wyoming, USA. *Geoderma* 59, 175–196.
- Dahms, D.E., Rawlins, C.L., 1996. A two-year record of eolian sedimentation in the Wind River range, Wyoming, U.S.A. *Arct. Alp. Res.* 28, 210–216.
- Dia, A., Chauvel, C., Bulourde, M., Gerard, M., 2006. Eolian contribution to soils on Mount Cameroon; isotopic and trace element records. *Chem. Geol.* 226, 232–252. <https://doi.org/10.1016/j.chemgeo.2005.09.022>.
- Dikshit, A., Pradhan, B., Huete, A., 2021. An improved SPEI drought forecasting approach using the long short-term memory neural network. *J. Environ. Manag.* 283, 111979. <https://doi.org/10.1016/j.jenvman.2021.111979>.
- Dymond, J., Biscaye, P.E., Rex, R.W., 1974. Eolian origin of mica in hawaiian soils. *Geol. Soc. Am. Bull.* 85, 37–40.
- Egan, P.A., Price, M.F., 2017. Mountain Ecosystem Services and Climate Change: A Global Overview of Potential Threats and Strategies for Adaptation.
- Froyd, K.D., Yu, P., Schill, G.P., Brock, C.A., Kupc, A., Williamson, C.J., Jensen, E.J., Ray, E., Rosenlof, K.H., Bian, H., 2022. Dominant role of mineral dust in cirrus cloud formation revealed by global-scale measurements. *Nat. Geosci.* 1–7.
- Gill, T.E., 1996. Eolian sediments generated by anthropogenic disturbance of playas: human impacts on the geomorphic system and geomorphic impacts on the human system. *Geomorphology* 17, 207–228.
- Goodman, M.M., Carling, G.T., Fernandez, D.P., Rey, K.A., Hale, C.A., Bickmore, B.R., Nelson, S.T., Munroe, J.S., 2019. Trace element chemistry of atmospheric deposition along the wasatch front (Utah, USA) reflects regional playa dust and local urban aerosols. *Chem. Geol.* 119317. <https://doi.org/10.1016/j.chemgeo.2019.119317>.
- Goudie, A., 2018. Dust storms and ephemeral lakes. *Desert* 23, 153–164.
- Grêt-Regamey, A., Weibel, B., 2020. Global assessment of mountain ecosystem services using earth observation data. *Ecosyst. Serv.* 46, 101213.
- Grêt-Regamey, A., Brunner, S.H., Kienast, F., 2012. Mountain ecosystem services: who cares? *Mt. Res. Dev.* 32.
- Hahnenberger, M., Nicoll, K., 2012. Meteorological characteristics of dust storm events in the eastern Great Basin of Utah, USA. *Atmos. Environ.* 60, 601–612.
- Hahnenberger, M., Nicoll, K., 2014. Geomorphic and land cover identification of dust sources in the eastern Great Basin of Utah, USA. *Geomorphology* 204, 657–672.
- Hahnenberger, M., Perry, K.D., 2015. Chemical comparison of dust and soil from the Sevier Dry Lake, UT, USA. *Atmos. Environ.* 113, 90–97.
- Hale, C.A., Carling, G.T., Nelson, S.T., Fernandez, D.P., Brooks, P.D., Rey, K.A., Tingey, D.G., Packer, B.N., Aanderud, Z.T., 2022. Strontium isotope dynamics reveal streamflow contributions from shallow flow paths during snowmelt in a montane watershed, Provo River, Utah, USA. *Hydrol. Process.* 36, e14458.
- Hamzeh, N.H., Kaskaoutis, D.G., Rashki, A., Mohammadpour, K., 2021. Long-term variability of dust events in southwestern Iran and its relationship with the drought. *Atmosphere* 12, 1350.
- Heindel, R.C., Putman, A.L., Murphy, S.F., Repert, D.A., Hinckley, E.-L.S., 2020. Atmospheric dust deposition varies by season and elevation in the Colorado front range, USA. *J. Geophys. Res. Earth Surf.* 125, e2019JF005436. <https://doi.org/10.1029/2019JF005436>.
- Kaufman, Y.J., Tanré, D., Dubovik, O., Karnieli, A., Remer, L.A., 2001. Absorption of sunlight by dust as inferred from satellite and ground-based remote sensing. *Geophys. Res. Lett.* 28, 1479–1482.
- Kim, D., Chin, M., Cruz, C.A., Tong, D., Yu, H., 2021. Spring dust in western North America and its interannual variability—understanding the role of local and transported dust. *J. Geophys. Res. Atmos.* 126, e2021JD035383.
- Kurtz, A.C., Derry, L.A., Chadwick, O.A., 2001. Accretion of asian dust to hawaiian soils; isotopic, elemental, and mineral mass balances. *Geochim. Cosmochim. Acta* 65, 1971–1983. [https://doi.org/10.1016/S0016-7037\(01\)00575-0](https://doi.org/10.1016/S0016-7037(01)00575-0).
- Lawrence, C.R., Neff, J.C., 2009. The contemporary physical and chemical flux of aeolian dust; a synthesis of direct measurements of dust deposition. *Chem. Geol.* 267, 46–63. <https://doi.org/10.1016/j.chemgeo.2009.02.005>.
- Lawrence, C.R., Painter, T.H., Landry, C.C., Neff, J.C., 2010. Contemporary geochemical composition and flux of aeolian dust to the San Juan Mountains, Colorado, United States. *J. Geophys. Res.* 115, G03007. <https://doi.org/10.1029/2009JG001077>.
- Lawrence, C.R., Neff, J.C., Farmer, G.L., 2011. The accretion of aeolian dust in soils of the San Juan Mountains, Colorado, USA. *J. Geophys. Res. Earth Surf.* 116, F02013. <https://doi.org/10.1029/2010JF001899>.
- Lawrence, C.R., Reynolds, R.L., Ketterer, M.E., Neff, J.C., 2013. Aeolian controls of soil geochemistry and weathering fluxes in high-elevation ecosystems of the Rocky Mountains, Colorado. *Geochim. Cosmochim. Acta* 107, 27–46.
- Litaor, M.I., 1987. The influence of eolian dust on the genesis of alpine soils in the Front Range, Colorado. *Soil Sci. Soc. Am. J.* 51, 142–147.
- Mahowald, N.M., Baker, A.R., Bergametti, G., Brooks, N., Duce, R.A., Jickells, T.D., Kubilay, N., Prospero, J.M., Tegen, I., 2005. Atmospheric global dust cycle and iron inputs to the ocean. *Glob. Biogeochem. Cycles* 19.
- Miller, M.E., Bowker, M.A., Reynolds, R.L., Goldstein, H.L., 2012. Post-fire land treatments and wind erosion—lessons from the Milford flat fire, UT, USA. *Aeolian Res.* 7, 29–44.
- Miller, O.L., Solomon, D.K., Fernandez, D.P., Cerling, T.E., Bowling, D.R., 2014. Evaluating the use of strontium isotopes in tree rings to record the isotopic signal of dust deposited on the Wasatch Mountains. *Appl. Geochem.* 50, 53–65.
- Muhs, D.R., Benedict, J.B., 2006. Eolian additions to late quaternary alpine soils, indian peaks wilderness area, Colorado front range. *Arct. Antarct. Alp. Res.* 38, 120–130.
- Munroe, J.S., 2006. Investigating the spatial distribution of summit flats in the Uinta Mountains of northeastern Utah, USA. *Geomorphology* 75, 437–449.
- Munroe, J.S., 2007. Properties of alpine soils associated with well-developed sorted polygons in the Uinta Mountains, Utah, USA. *Arct. Antarct. Alp. Res.* 39, 578–591.
- Munroe, J.S., 2014. Properties of modern dust accumulating in the Uinta Mountains, Utah, USA, and implications for the regional dust system of the Rocky Mountains. *Earth Surf. Process. Landf.* 39, 1979–1988.
- Munroe, J.S., Laabs, B.J.C., 2009. Glacial Geologic Map of the Uinta Mountains Area, Utah and Wyoming. Utah Geological Survey Miscellaneous Publication 09-4DM.
- Munroe, J.S., Attwood, E.C., O'Keefe, S.S., Quackenbush, P.J., 2015. Eolian deposition in the alpine zone of the Uinta Mountains, Utah, USA. *Catena* 124, 119–129.
- Munroe, J.S., Norris, E.D., Carling, G.T., Beard, B.L., Satkoski, A.M., Liu, L., 2019. Isotope fingerprinting reveals western north american sources of modern dust in the Uinta Mountains, Utah, USA. *Aeolian Res.* 38, 39–47.
- Munroe, J.S., Norris, E.D., Olson, P.M., Ryan, P.C., Tappa, M.J., Beard, B.L., 2020. Quantifying the contribution of dust to alpine soils in the periglacial zone of the Uinta Mountains, Utah, USA. *Geoderma* 378, 114631.
- Munroe, J.S., McElroy, R., O'Keefe, S., Peters, A., Wasson, L., 2021. Holocene records of eolian dust deposition from high-elevation lakes in the Uinta Mountains, Utah, USA. *J. Quat. Sci.* 36, 66–75.
- Munroe, J.S., Ryan, P.C., Proctor, A., 2021. Pedogenic clay formation from allochthonous parent materials in a periglacial alpine critical zone. *Catena* 203, 105324.
- National Research Council, 2001. Basic Research Opportunities in Earth Science. The National Academies Press, Washington, DC <https://doi.org/10.17226/9981>.
- Neff, J.C., Ballantyne, A.P., Farmer, G.L., Mahowald, N.M., Conroy, J.L., Landry, C.C., Overpeck, J.T., Painter, T.H., Lawrence, C.R., Reynolds, R.L., 2008. Increasing eolian dust deposition in the western United States linked to human activity. *Nat. Geosci.* 1, 189–195. <https://doi.org/10.1038/ngeo133>.
- Neff, J.C., Reynolds, R.L., Munson, S.M., Fernandez, D., Belnap, J., 2013. The role of dust storms in total atmospheric particle concentrations at two sites in the western US. *J. Geophys. Res. Atmos.* 118, 11–201.
- Nicoll, K., Hahnenberger, M., Goldstein, H.L., 2020. 'Dust in the wind' from source-to-sink: analysis of the 14–15 april 2015 storm in Utah. *Aeolian Res.* 46, 100532.
- Painter, T.H., Barrett, A.P., Landry, C.C., Neff, J.C., Cassidy, M.P., Lawrence, C.R., McBride, K.E., Farmer, G.L., 2007. Impact of disturbed desert soils on duration of mountain snow cover. *Geophys. Res. Lett.* 34. <https://doi.org/10.1029/2007GL030284> L12502-L12502.
- Painter, T.H., Deems, J.S., Belnap, J., Hamlet, A.F., Landry, C.C., Udall, B., 2010. Response of Colorado River runoff to dust radiative forcing in snow. *Proc. Natl. Acad. Sci.* 107, 17125–17130.
- Pourmand, A., Prospero, J.M., Sharifi, A., 2014. Geochemical fingerprinting of trans-Atlantic african dust based on radiogenic sr-and-hf isotopes and rare earth element anomalies. *Geology* 42, 675–678.
- Prospero, J.M., 1999. Long-range transport of mineral dust in the global atmosphere: impact of african dust on the environment of the southeastern United States. *Proc. Natl. Acad. Sci.* 96, 3396–3403.
- Prospero, J.M., Lamb, P.J., 2003. African droughts and dust transport to the Caribbean: climate change implications. *Science* 302, 1024–1027.
- Prospero, J.M., Nees, R.T., 1977. Dust concentration in the atmosphere of the equatorial North Atlantic: possible relationship to the sahelian drought. *Science* 196, 1196–1198.
- Psenner, R., 1999. Living in a dusty world: airborne dust as a key factor for Alpine lakes. *Water Air Soil Pollut.* 112, 217–227. <https://doi.org/10.1023/A:1005082832499>.
- Rea, P., Ma, L., Gill, T.E., Gardea-Torresdey, J., Tamez, C., Jin, L., 2020. Tracing gypsiferous White Sands aerosols in the shallow critical zone in the northern Sacramento Mountains, New Mexico using Sr/Ca and 87Sr/86Sr ratios. *Geoderma* 372, 114387.
- Reheis, M.C., 1997. Dust deposition downwind of Owens (dry) Lake, 1991–1994: preliminary findings. *J. Geophys. Res. Atmos.* 102, 25999–26008.
- Reheis, M.C., Kihl, R., 1995. Dust deposition in southern Nevada and California, 1984–1989: relations to climate, source area, and source lithology. *J. Geophys. Res.* 100, 8893–8918.
- Reynolds, R.L., Yount, J.C., Reheis, M., Goldstein, H., Chavez, P., Fulton, R., Whitney, J., Fuller, C., Forester, R.M., 2007. Dust emission from wet and dry playas in the Mojave Desert, USA. *Earth Surf. Process. Landf.* 32, 1811–1827.
- Reynolds, R.L., Mordecai, J.S., Rosenbaum, J.G., Ketterer, M.E., Walsh, M.K., Moser, K.A., 2010. Compositional changes in sediments of subalpine lakes, Uinta Mountains (Utah): evidence for the effects of human activity on atmospheric dust inputs. *J. Paleolimnol.* 44, 161–175.
- Reynolds, R.L., Goldstein, H.L., Moskowicz, B.M., Bryant, A.C., Skiles, S.M., Kokaly, R.F., Flagg, C.B., Yauk, K., Berquó, T., Breit, G., 2013. Composition of dust deposited to snow cover in the wasatch range (Utah, USA): controls on radiative properties of snow cover and comparison to some dust-source sediments. *Aeolian Res.* 15, 73–90.
- Routson, C.C., Arcusa, S.H., McKay, N.P., Overpeck, J.T., 2019. A 4,500-year-long record of southern Rocky Mountain dust deposition. *Geophys. Res. Lett.* 46, 8281–8288. <https://doi.org/10.1029/2019GL083255>.
- Scholz, J., Brahney, J., 2022. Evidence for multiple potential drivers of increased phosphorus in high-elevation lakes. *Sci. Total Environ.* 825, 153939.

- Seager, R., Ting, M., Held, I., Kushnir, Y., Lu, J., Vecchi, G., Huang, H.-P., Harnik, N., Leetmaa, A., Lau, N.-C., 2007. Model projections of an imminent transition to a more arid climate in southwestern North America. *Science* 316, 1181–1184.
- Seager, R., Ting, M., Li, C., Naik, N., Cook, B., Nakamura, J., Liu, H., 2013. Projections of declining surface-water availability for the southwestern United States. *Nat. Clim. Chang.* 3, 482–486.
- Shao, Y., 2001. A model for mineral dust emission. *J. Geophys. Res. Atmos.* 106, 20239–20254.
- Shao, Y., Lu, H., 2000. A simple expression for wind erosion threshold friction velocity. *J. Geophys. Res. Atmos.* 105, 22437–22443. <https://doi.org/10.1029/2000JD900304>.
- Shao, Y., Wyrwoll, K.-H., Chappell, A., Huang, J., Lin, Z., McTainsh, G.H., Mikami, M., Tanaka, T.Y., Wang, X., Yoon, S., 2011. Dust cycle: an emerging core theme in earth system science. *Aeolian Res.* 2, 181–204.
- Skiles, S.M., Painter, T.H., Belnap, J., Holland, L., Reynolds, R.L., Goldstein, H.L., Lin, J., 2015. Regional variability in dust-on-snow processes and impacts in the upper Colorado River basin. *Hydrol. Process.* 29, 5397–5413.
- Skiles, S.M., Mallia, D.V., Hallar, A.G., Lin, J.C., Lambert, A., Petersen, R., Clark, S., 2018. Implications of a shrinking great salt Lake for dust on snow deposition in the Wasatch Mountains, UT, as informed by a source to sink case study from the 13–14 april 2017 dust event. *Environ. Res. Lett.* 13, 124031.
- Sow, M., Goossens, D., Rajot, J.L., 2006. Calibration of the MDCO dust collector and of four versions of the inverted frisbee dust deposition sampler. *Geomorphology* 82, 360–375. <https://doi.org/10.1016/j.geomorph.2006.05.013>.
- Steenburgh, W.J., Massey, J.D., Painter, T.H., 2012. Episodic dust events of Utah's wasatch front and adjoining region. *J. Appl. Meteorol. Climatol.* 51, 1654–1669.
- Stuut, J.-B., Smalley, I., O'Hara-Dhand, K., 2009. Aeolian dust in Europe: african sources and european deposits. *Quat. Int.* 198, 234–245.
- Tau, G., Crouvi, O., Enzel, Y., Teutsch, N., Ginoux, P., Rasmussen, C., 2021. Shutting down dust emission during the middle holocene drought in the Sonoran Desert, Arizona, USA. *Geology* 49, 857–861.
- Thorn, C.E., Darmody, R.G., 1980. Contemporary eolian sediments in alpine zone, Colorado front range. *Phys. Geogr.* 1, 162–171.
- Tobo, Y., Adachi, K., DeMott, P.J., Hill, T.C., Hamilton, D.S., Mahowald, N.M., Nagatsuka, N., Ohata, S., Uetake, J., Kondo, Y., 2019. Glacially sourced dust as a potentially significant source of ice nucleating particles. *Nat. Geosci.* 12, 253–258.
- Tsai, H., Chen, J.-H., Huang, W.-S., Huang, S.-T., Hseu, Z.-Y., You, C.-F., 2021. Aeolian additions of podzolic soils on the high-altitude mountains in Central Taiwan-sediment origin and pedological implications. *Geoderma* 383, 114726.
- VanCuren, R.A., Cahill, T.A., 2002. Asian aerosols in North America: frequency and concentration of fine dust. *J. Geophys. Res. Atmos.* 107.
- Vandenbergh, J., 2013. Grain size of fine-grained windblown sediment: a powerful proxy for process identification. *Earth-Sci. Rev.* 121, 18–30.
- Wagenbach, D., Preunkert, S., Schäfer, J., Jung, W., Tomadin, L., 1996. Northward transport of Saharan dust recorded in a deep Alpine ice core. *The Impact of Desert Dust Across the Mediterranean*. Springer, pp. 291–300.
- Wang, Y., Xie, Y., Dong, W., Ming, Y., Wang, J., Shen, L., 2017. Adverse effects of increasing drought on air quality via natural processes. *Atmos. Chem. Phys.* 17, 12827–12843.
- Watson, A., 1992. Desert soils. *Developments in Earth Surface Processes*. Elsevier, pp. 225–260.
- Wedepohl, K.H., 1995. The composition of the continental crust. *Geochim. Cosmochim. Acta* 59, 1217–1232.
- Wesley, M.L., Hicks, B.B., 2000. A review of the current status of knowledge on dry deposition. *Atmos. Environ.* 34 (12), 2261–2282.
- Williams, A.P., Cook, B.I., Smerdon, J.E., 2022. Rapid intensification of the emerging southwestern north american megadrought in 2020–2021. *Nat. Clim. Chang.* 12, 232–234.
- Wilshire, H.G., 1983. The impact of vehicles on desert soil stabilizers. *Environmental Effects of Off-Road Vehicles*. Springer, pp. 31–50.
- Wurtsbaugh, W.A., Miller, C., Null, S.E., DeRose, R.J., Wilcock, P., Hahnenberger, M., Howe, F., Moore, J., 2017. Decline of the world's saline lakes. *Nat. Geosci.* 10, 816.
- Yaalon, D.H., Ganor, E., 1973. The influence of dust on soils during the quaternary. *Soil Sci.* 116, 146–155.
- Zhai, P., Pirani, A., Connors, S., Péan, C., Berger, S., Caud, N., Chen, Y., Goldfarb, L., Gomis, M., Huang, M., 2021. IPCC 2021: Climate Change 2021: The Physical Science Basis. Contribution of Working Group I to the Sixth Assessment Report of the Intergovernmental Panel on Climate Change.
- Zhao, W., Balsam, W., Williams, E., Long, X., Ji, J., 2018. Sr–Nd–Hf isotopic fingerprinting of transatlantic dust derived from North Africa. *Earth Planet. Sci. Lett.* 486, 23–31.
- Zoljoodi, M., Didevarasl, A., Saadatabadi, A.R., 2013. Dust Events in the Western Parts of Iran and the Relationship With Drought Expansion Over the Dust-source Areas in Iraq and Syria.